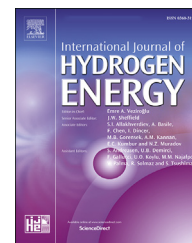


Available online at [www.sciencedirect.com](http://www.sciencedirect.com)

ScienceDirect

journal homepage: [www.elsevier.com/locate/he](http://www.elsevier.com/locate/he)

# Comparison of reduction kinetics of $\text{Fe}_2\text{O}_3$ , $\text{ZnOFe}_2\text{O}_3$ and $\text{ZnO}$ with hydrogen ( $\text{H}_2$ ) and carbon monoxide ( $\text{CO}$ )



Ulrich Brandner\*, Manuel Leuchtenmueller

Chair of Nonferrous Metallurgy, Montanuniversität Leoben, Franz-Josef-Strasse 18, 8700 Leoben, Austria

## HIGHLIGHTS

- The kinetical advantage of  $\text{H}_2$  compared to  $\text{CO}$  is the most pronounced for  $\text{Fe}_2\text{O}_3$  and decreases for  $\text{ZnOFe}_2\text{O}_3$  and  $\text{ZnO}$ .
- The temperature dependency for both reducing agent is only visible for  $\text{ZnO}$ . for the entire experiment.
- Within the applied temperature (800–900 °C) both reducing agents only show a marginal temperature dependency for  $\text{Fe}_2\text{O}_3$ .
- $\text{Fe}_2\text{O}_3$  reduction was found to be controlled by diffusion and  $\text{ZnO}$  reduction was found to be controlled by chemical reaction.
- Doubling of gas flow leads to a doubled reduction rate. Quadrupling of the gas flow results in a tripled reduction rate.

## ARTICLE INFO

### Article history:

Received 29 November 2022

Received in revised form

25 June 2023

Accepted 17 July 2023

Available online 02 August 2023

### Keywords:

Electric arc furnace dust (EAFD)

Hydrogen reduction

Kinetics

$\text{CO}_2$ -Reduction

Thermogravimetric analysis (TGA)

## ABSTRACT

Electric arc furnace dust (EAFD) recycling is based on the reduction of oxides containing iron and zinc. With regard to the sustainability of industrial processes, hydrogen reduction processes could be the key technology to replace current recycling technologies based on carbothermal reduction. In this context, hydrogen is often claimed to provide better reduction kinetics, but it is mostly unclear how much faster it is. The present work gives a comprehensive comparison of the reduction kinetics of the major zinc- and iron-containing oxides in EAFD ( $\text{Fe}_2\text{O}_3$ ,  $\text{ZnOFe}_2\text{O}_3$ , and  $\text{ZnO}$ ) using hydrogen and carbon monoxide under various process parameters. The influence of specimen size, reduction gas flow rate, and temperature were evaluated. The kinetic advantage of hydrogen compared to carbon monoxide was confirmed, enabling the reduction of direct  $\text{CO}_2$ -emission. Hydrogen results in a 2.5 times faster reduction of  $\text{Fe}_2\text{O}_3$  and a doubling of the reduction rate for  $\text{ZnOFe}_2\text{O}_3$ .  $\text{ZnO}$  reduction was determined to be 1.5 faster. Furthermore,  $\text{ZnO}$  was found to be the rate-limiting substance in the recycling of EAFD, regardless of the reducing agent.

© 2023 The Authors. Published by Elsevier Ltd on behalf of Hydrogen Energy Publications LLC. This is an open access article under the CC BY license (<http://creativecommons.org/licenses/by/4.0/>).

## 1. Introduction

The iron and steel industry is currently responsible for 7.2% of the global carbon dioxide emissions [1]. Due to the projected increase in steel demand of 33% by 2050, carbon dioxide

emissions from the steel industry will continue to increase. Steel production by electric arc furnace will more than double from the global production capacity of 517 million tons in 2019 to 1200 million tons in 2050 [2,3]. In addition to the direct carbon dioxide emissions, steel production via the electric arc furnace (EAF) generates about 15–25 kg of hazardous electric

\* Corresponding author.

E-mail addresses: [ulrich.brandner@gmx.at](mailto:ulrich.brandner@gmx.at) (U. Brandner), [manuel.leuchtenmueller@unileoben.ac.at](mailto:manuel.leuchtenmueller@unileoben.ac.at) (M. Leuchtenmueller).

<https://doi.org/10.1016/j.ijhydene.2023.07.189>

0360-3199/© 2023 The Authors. Published by Elsevier Ltd on behalf of Hydrogen Energy Publications LLC. This is an open access article under the CC BY license (<http://creativecommons.org/licenses/by/4.0/>).

arc furnace dust (EAFD) per ton of steel [4]. Due to the increasing production capacities, the amount of EAFD produced worldwide will increase from 8 million tons per year to 18 million tons by 2050 [5].

Currently, the best available technique for processing EAFD is the Waelz process, which is based on carbothermal reduction of the zinc oxidic in EAFD [6,7]. This treatment process emits a significant amount of carbon dioxide emissions, which are also expected to increase. Therefore, green steel production must also include alternative process concepts to treat EAFD [8]. A promising way to accomplish the task to decrease direct CO<sub>2</sub>-emissions is to use hydrogen as a reducing agent for the contained oxides [5]. In this context, hydrogen is often described to provide better reaction kinetics than carbon monoxide [9–14]. Zuo et al. made reduction experiments of iron ore with mixtures of carbon monoxide and hydrogen and the kinetics improved by the increase of the share of hydrogen [15]. Different works of Tong et al. allows the implication of the reduction kinetics at 800 °C for zinc ferrite with hydrogen and carbon monoxide [10,12].

However, a direct comparison of the reduction kinetics between hydrogen and carbon monoxide in the scope of EAFD recycling is yet not available.

The present work aims to fill this gap and provide a well-founded direct comparison of the reduction kinetics of hydrogen with carbon monoxide for the main reducible components of EAFD [16]: iron oxide (Fe<sub>2</sub>O<sub>3</sub>), zinc ferrite (ZnO) and zinc ferrite (ZnOFe<sub>2</sub>O<sub>3</sub>).

## 2. Materials and methods

### 2.1. Materials

The following pure substances in powder form were used for the kinetic study.

- Iron oxide: Fe<sub>2</sub>O<sub>3</sub> (purity: >98%)
- Zinc ferrite: ZnOFe<sub>2</sub>O<sub>3</sub> (purity: >99%)
- Zinc oxide: ZnO (purity: >99%)

Fe<sub>2</sub>O<sub>3</sub> and ZnOFe<sub>2</sub>O<sub>3</sub> were provided by Alfa Aesar GmbH & Co KG and ZnO by Carl Roth GmbH. To remove any residual moisture and ensure the highest possible oxidation state of the oxides, all materials were calcined for 24 h at 900 °C under oxidizing conditions in a laboratory muffle furnace.

### 2.2. Experimental setup

Fig. 1a shows a sketch of the Linseis Pt 1600 thermogravimetric analyzer (TGA), which is explained in detail in Ref. [17]. The TGA is equipped with a gas supply unit consisting of mass flow controllers for the reduction gas (hydrogen or carbon monoxide) and the load cell chamber (nitrogen). Both gases are fed to the furnace chamber with the specimen. The reduction gas thus consists of a mixture of hydrogen or carbon monoxide and nitrogen. The nitrogen flow.

Fig. 1b shows the setup inside the sample chamber. The respective oxide was pressed into a cylindrical specimen, which had either a mass of 300 mg and a diameter of 6 mm or 600 mg and 7.5 mm. The furnace was heated under a pure nitrogen atmosphere to the target temperature as shown in Table 1. Each trial was started by either introducing hydrogen or carbon monoxide into the furnace chamber. The subsequent reduction causes a mass decrease according to the following chemical reactions:

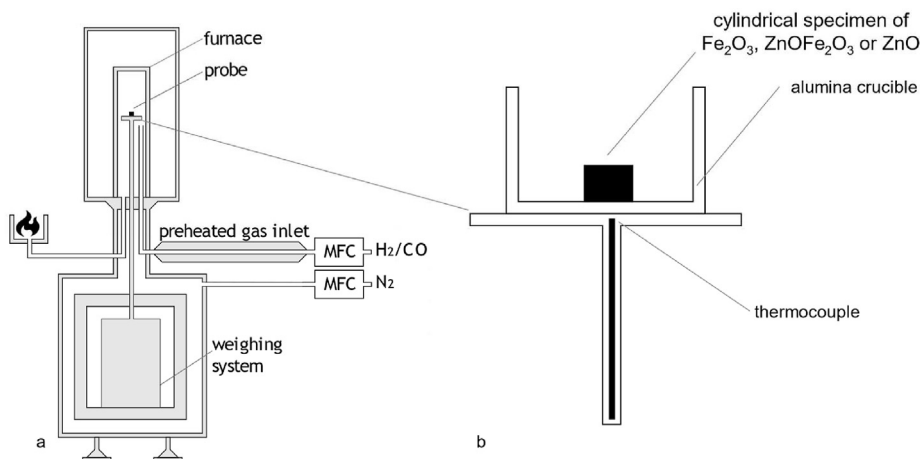
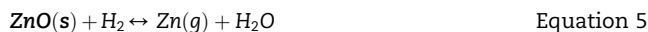
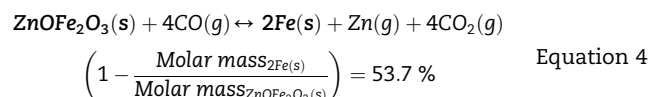
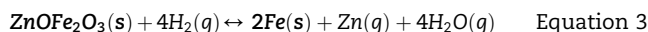
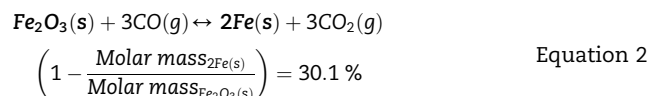
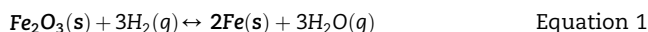
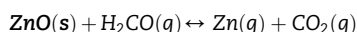


Fig. 1 – Experimental setup: (a) TGA instrument (Linseis PT1600), (b) experimental setup in specimen chamber.

**Table 1 – Overview of the conducted trial settings.**

Material	Specimen weight [mg]	Purge gas	Purge gas flow [ml/min]	Reducing gas	Reducing gas flow [ml/min]	Reducing gas concentration [vol%]	Temperature [°C]
Fe <sub>2</sub> O <sub>3</sub>	300	N <sub>2</sub>	100	H <sub>2</sub>	280	73.7	800
ZnOFe <sub>2</sub> O <sub>3</sub>				CO			850
ZnO				900			
	300				280	73.7	800
	600				140	58.3	
					70	41.2	



Equation 6

Equation (1) and Equation (2) indicate that a theoretical achievable complete reduction of Fe<sub>2</sub>O<sub>3</sub> equals a mass decrease of 30.1%, a complete reduction of ZnOFe<sub>2</sub>O<sub>3</sub> leads to a mass decrease of 53.7% (Equation (3) and Equation (4)) and a complete reduction of ZnO leads to a mass decrease of 100% (Equation (5) and Equation (6)). Within this work the reduction behavior of the oxides with carbon monoxide and hydrogen were tested by varying the sample size, the gas flow or reducing gas concentration and the temperature. Table 1 summarizes the parameters of the conducted thermogravimetric analyses. The maximum reducing gas flow of 280 ml/min was the highest adjustment of the mass flow controllers of the TGA instrument. This setting allows for the highest possible reaction rate. The gas flow was reduced by factors of 2–140 l/min and 4–70 l/min. The set temperature values were chosen in order to conduct experiments in a temperature range possibly for an industrial reduction process for EAFD with hydrogen. The range of the temperature was chosen very narrow to ensure the reduction mechanism only changes marginally as a function of the temperature. Furthermore, the set temperature range of our experiments was chosen, because between 800° and 900 °C all stability regions of Fe and Zn and corresponding oxides are possible depending on the gas composition of reducing gas atmosphere (see also Fig. 13) [5]. For Zn the stability region is additionally a function of the partial pressure of the reduced zinc [5].

### 2.3. Surface measurement via the BET method

The specific surface areas (SSA) of selected specimens (300 mg) were measured via the BET-method in a Quantachrome Nova 2000e - Surface Area & Pore Size Analyzer [18]. Table 2 shows the results of measurements for Fe<sub>2</sub>O<sub>3</sub>, ZnOFe<sub>2</sub>O<sub>3</sub> and ZnO for the initial state prior to the

**Table 2 – Specific surface area of initial and reduced specimens determined via the BET method.**

Substance	Specific surface area [m <sup>2</sup> /g]/[%]		
	initial state (calcinated)	after H2 reduction at 900 °C	after CO reduction at 900 °C
Fe <sub>2</sub> O <sub>3</sub>	3.45	1.44/(41.7)	0.35/(10.1)
ZnOFe <sub>2</sub> O <sub>3</sub>	3.39	2.85/(84.0)	1.15/(33.9)
ZnO	5.08	–	–

thermogravimetric experiments. While Fe<sub>2</sub>O<sub>3</sub> and ZnOFe<sub>2</sub>O<sub>3</sub> exhibit a similar SSA, the SSA of ZnO is significantly higher. Table 2 also displays the SSA of Fe<sub>2</sub>O<sub>3</sub> and ZnO·Fe<sub>2</sub>O<sub>3</sub> after the reduction in the TGA with hydrogen and carbon monoxide at the highest experimental temperature. Additionally, the ratio to the initial SSA is displayed. The highest temperature was chosen to gain the highest probability of the decrease of the specific surface area. Both reducing agents decrease the specific surface area for Fe<sub>2</sub>O<sub>3</sub> and ZnO·Fe<sub>2</sub>O<sub>3</sub>. The decrease cause by carbon monoxide and for Fe<sub>2</sub>O<sub>3</sub> is greater.

### 2.4. Data evaluation method

The thermogravimetric analyzer determines the mass decrease of the specimen in mg over time. Fig. 2a shows the mass signals from two exemplary experiments. Since the input mass of each experiment varies in a certain range around 300 mg and 600 mg, respectively, and the reduction of the oxides causes different relative mass decreases, it is advisable to convert the mass decrease from absolute values to a relative degree of reduction according to Equation (7). Fig. 2b shows the reduction degree of the two example experiments as a function of time.

$$\text{Reduction Degree} = \frac{\Delta m(t)}{\Delta[\%]_{\text{oxide}} \cdot m_0} \cdot 100[\%]$$

$$\Delta m(t) \dots \text{measured mass decreases} / [\text{mg}]$$

$$\Delta[\%]_{\text{Fe}_2\text{O}_3} = 30.1 \%$$

$$\Delta[\%]_{\text{ZnO} \cdot \text{Fe}_2\text{O}_3} = 53.7 \%$$

$$\Delta[\%]_{\text{ZnO}} = 100 \%$$

Equation 7

$m_0 \dots$ input weight of the specimen (300 [mg] ±5 [mg]/600 [mg] ±10 [mg])

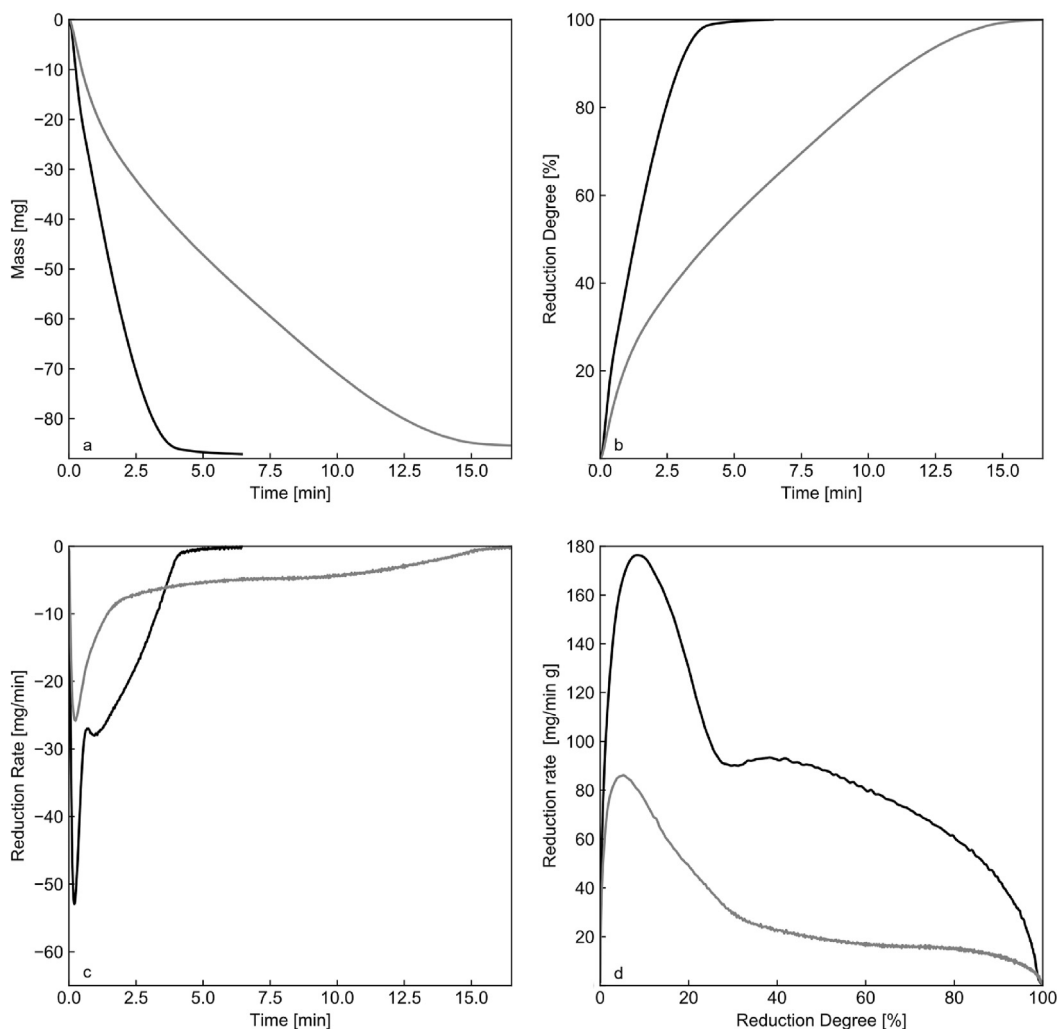


**Fig. 2** – (a) Time dependent mass signal of the TGA; (b) Reduction degree (0–100%) as a function of time; (c) Reduction rate (mg/min) as function of time; (d) Normalized reduction rate (mg/min g) as function of the reduction degree.

The numerical differentiation of the mass signal according to Equation (8) gives the reduction rate in mg/min [19,20].

$$\text{Reduction Rate} = \frac{m(t)_{n+1} - m(t)_n}{t_{n+1} - t_n} \cdot 100[\%]$$

$m(t)_{n+1}$ ...measured mass signal related to time step  $t_{n+1}$ / [mg]

$m(t)_n$ ...measured mass signal related to time step  $t_n$ / [mg]

Equation 8

Fig. 2c shows the reduction rate as a function of time. Normalizing the reduction rate with respect to the sample mass and plotting the reduction rate as a function of reduction ratio allows to directly compare different experimental conditions, as shown in Fig. 2d. The results listed below are shown in Fig. 2d.

Furthermore, calculating the reduction rate ratio as a function of the degree of reduction degree according to Equation (9) improves the comparability of the different experiments and allows further conclusions.

$$\text{Reduction rate ratio} = \frac{\text{Reduction rate of trial}}{\text{Reduction rate of reference}} \quad \text{Equation 9}$$

### 3. Experimental results and discussion

#### 3.1. Reduction rate as function of the reduction degree comparison

The reduction behavior was tested under various process parameters. Fig. 3 summarizes the temperature influence on the reduction rate between 800, 850, and 900 °C.

It shows that hydrogen results in a higher reduction rate than carbon monoxide. The temperature influence increases from  $\text{Fe}_2\text{O}_3$  via  $\text{ZnOFe}_2\text{O}_3$  to  $\text{ZnO}$ . The reduction of  $\text{Fe}_2\text{O}_3$  consists of multiple reaction steps, which is visible by the initial peak which maps the Hematite ( $\text{Fe}_2\text{O}_3$ ) to Magnetite ( $\text{Fe}_3\text{O}_4$ ) and Wuestite ( $\text{FeO}$ ) reduction. Compared to that,  $\text{ZnO}$

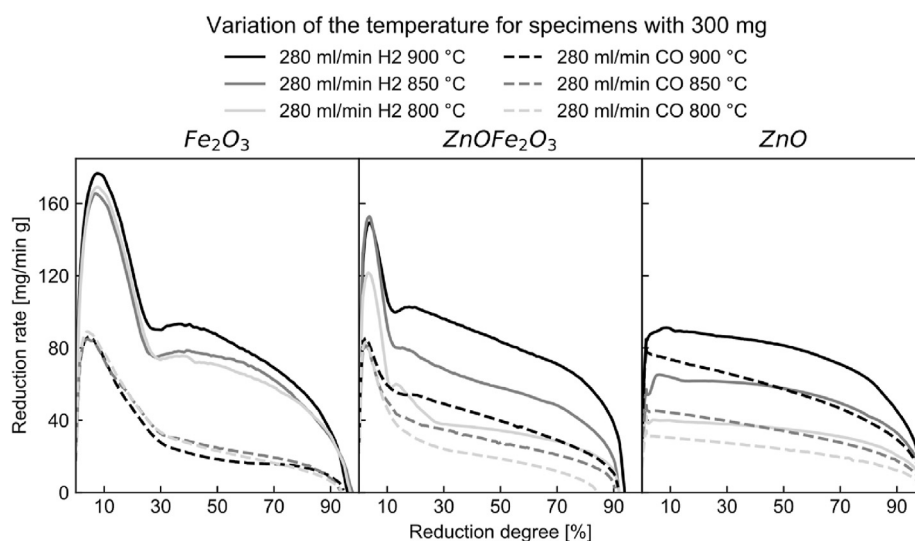


**Fig. 3** – Normalized reduction rate as a function of the reduction degree for 300 mg  $\text{Fe}_2\text{O}_3$ ,  $\text{ZnOFe}_2\text{O}_3$  and  $\text{ZnO}$  with 280 ml/min hydrogen or carbon monoxide at varying temperature.

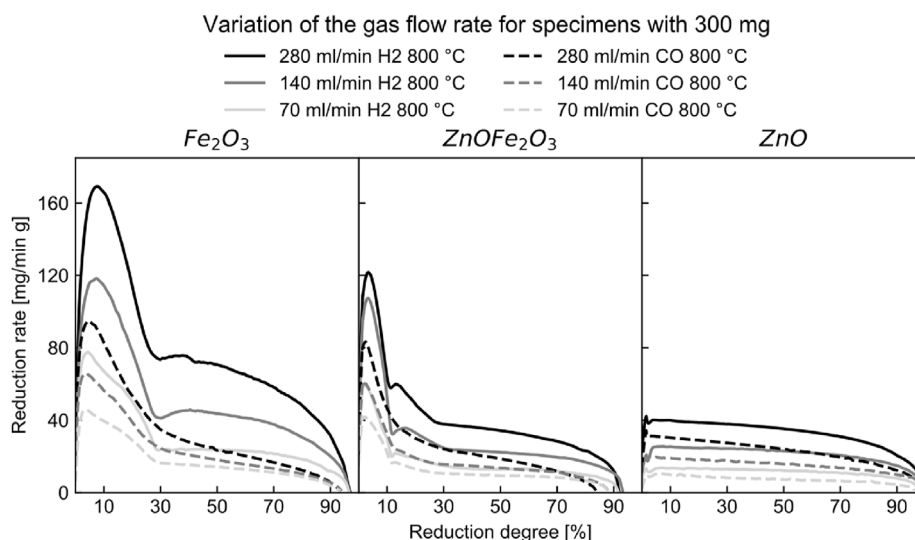


**Fig. 4** – Normalized reduction rate as a function of the reduction degree for 300 mg  $\text{Fe}_2\text{O}_3$ ,  $\text{ZnOFe}_2\text{O}_3$  and  $\text{ZnO}$  with a varying hydrogen or carbon monoxide flow rate at 800 °C.

reduction is a single-step reaction showing a relatively constant reaction rate [21–26]. This indicates that the gas surrounding the specimen gets saturated with zinc vapor, which decreases the reduction rate towards the end of the experiments. Especially due to the relatively low reduction temperature of all conducted experiments this effect is significantly, which is in line with the thermodynamic calculation of Reference [5].

Fig. 4 outlines the influence of the gas flow on the reaction rate for 300 mg specimens. Flow rates of 70, 140 and 280 ml/min were tested. It shows that the gas flow rate significantly influences the reaction rate with a higher flow increasing the kinetics. A higher flow means that the concentrations of reaction products ( $\text{H}_2\text{O}$ ,  $\text{CO}_2$ ) are lower levels resulting in a higher concentration of hydrogen or carbon monoxide which increases the number of occurring collisions and therefore

also the number of successful collisions. It additionally increases the concentration gradient from the reaction zone accumulating reaction products to the surrounding gas atmosphere, resulting in higher bulk diffusion rates. Additionally, less reaction products means a higher reduction potential which possibly also influences the reaction rates.

Fig. 5 shows the influence of the gas flow rate on the reaction rate for 600 mg specimens. The investigated flow rates were 70, 140, and 280 ml/min. The overall tendency is similar to Fig. 4, but with lower reaction rates. Comparing the highest detected reaction rate in Figs. 4 and 5, the relative reaction rate halves. Comparing the 280 ml/min and 600 mg with the 140 ml/min and 300 mg setup shows nearly identical relative reaction rates. The relative gas flow is in both cases 0.46 ml/(min mg). This means the main reason for the lower kinetics are the lowered relative gas flow rates. This effect illustrates

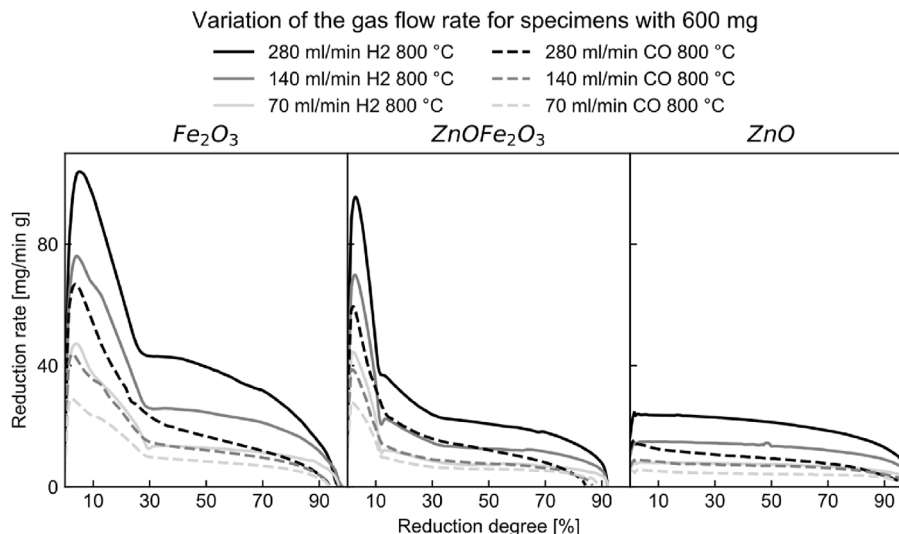


**Fig. 5** – Normalized reduction rate as a function of the reduction degree for 600 mg  $\text{Fe}_2\text{O}_3$ ,  $\text{ZnOFe}_2\text{O}_3$  and  $\text{ZnO}$  with a varying hydrogen or carbon monoxide flow rate at 800 °C.

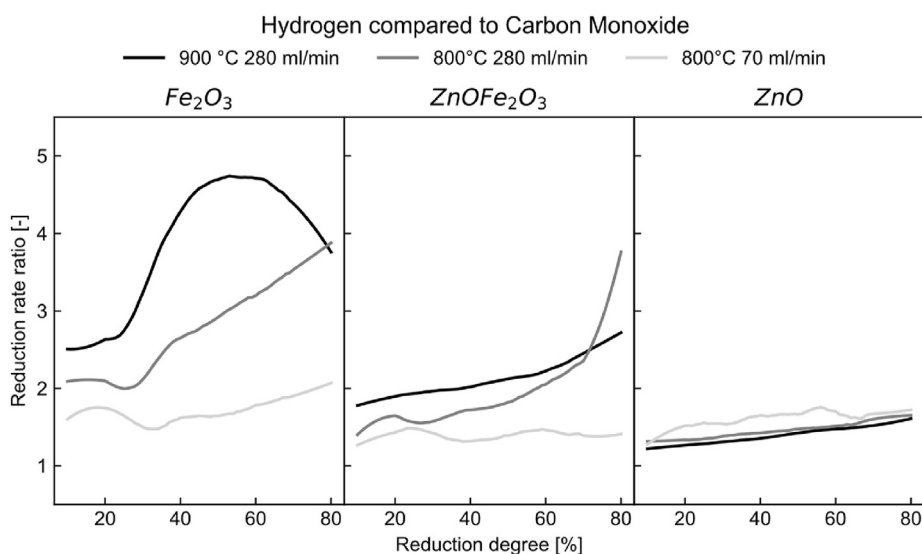


**Fig. 6** – Comparison of hydrogen and carbon monoxide for 300 mg  $\text{Fe}_2\text{O}_3$ ,  $\text{ZnOFe}_2\text{O}_3$  and  $\text{ZnO}$ .

the importance of the ratio between gas flow and sample size in thermogravimetric analyses when investigating solid-gas reduction reactions. In particular, previous work dealing with the reduction kinetics of oxides in EAFD was limited by the gas flow rate and the feed of the reducing agent [13,27–30].

### 3.2. Reduction rate ratio as function of the reduction degree comparison

Fig. 6 shows the ratio of the reduction rates of hydrogen with carbon monoxide being the reference at different temperatures and gas flow rates. The reduction rate ratio is most pronounced for  $\text{Fe}_2\text{O}_3$ , decreases for  $\text{ZnOFe}_2\text{O}_3$ , and is lowest for  $\text{ZnO}$ . The reduction rate ratio increases for all oxides at higher reduction levels. This effect is due to the higher diffusion rate of hydrogen compared to carbon monoxide. In

Ref. [31] a similar statement is given for  $\text{Fe}_2\text{O}_3$ , which also exhibits the highest pronouncement of this effect. In the case of  $\text{Fe}_2\text{O}_3$  and  $\text{ZnOFe}_2\text{O}_3$ , increasing the temperature and gas flow rate improves the kinetic advantage of hydrogen. In the case of  $\text{ZnO}$ , the course of the reduction rate ratio is independent of the temperature or the increase of the gas flow rate.

Fig. 7 compares the ratio of the reduction rate of hydrogen at different temperatures.  $\text{Fe}_2\text{O}_3$  shows the least influence of the temperature increase. Increasing the temperature improves the reduction kinetics of  $\text{ZnOFe}_2\text{O}_3$ , especially at a reduction degree above 30%.  $\text{ZnO}$  is reduced faster throughout the experiment by increasing the temperature. In particular, the smooth transition of the respective line from  $\text{Fe}_2\text{O}_3$  to  $\text{ZnOFe}_2\text{O}_3$  to  $\text{ZnO}$  shows the reduction transitions from  $\text{Fe}_2\text{O}_3$  reduction to  $\text{ZnO}$  reduction with increasing reduction degree within  $\text{ZnOFe}_2\text{O}_3$ .

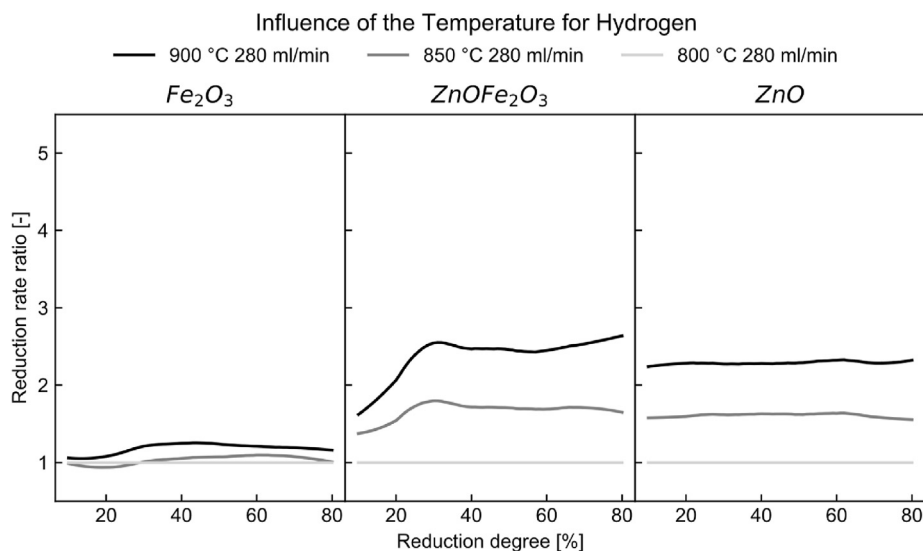


Fig. 7 – Influence of a temperature increase on the reduction of 300 mg  $Fe_2O_3$ ,  $ZnOFe_2O_3$  and  $ZnO$  with hydrogen.

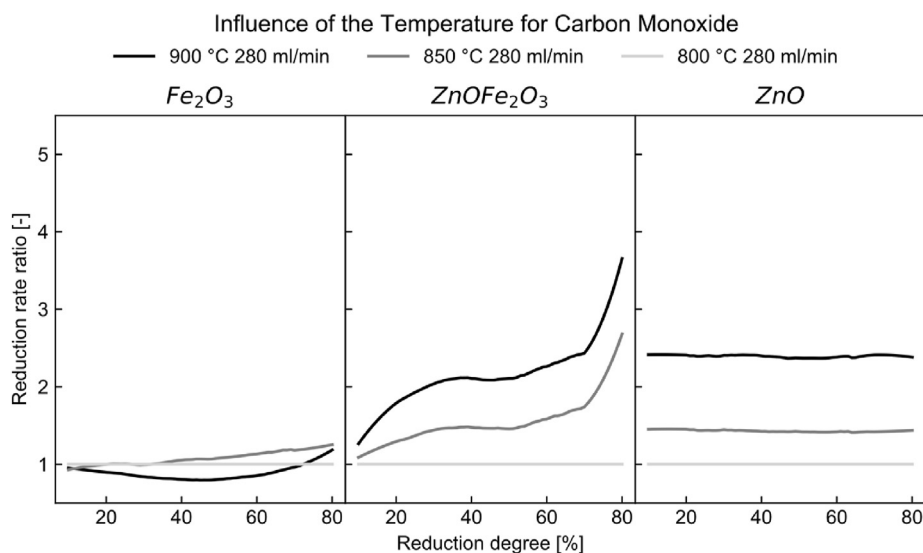


Fig. 8 – Influence of a temperature increase on the reduction of 300 mg  $Fe_2O_3$ ,  $ZnOFe_2O_3$  and  $ZnO$  with carbon monoxide.

Fig. 8 shows the influence of temperature on the reduction with carbon monoxide. A similar trend can be derived as for the reduction with hydrogen.

Fig. 9 shows the influence of the hydrogen gas flow rate. Except at the beginning of the reduction of  $Fe_2O_3$ , all oxides show a similar tendency. Doubling the hydrogen gas flow rate from 70 ml/min to 140 ml/min results in a doubling of the reduction rate. Further doubling to 280 ml/min, which corresponds to a fourfold increase relative to 70 ml/min, leads to only a threefold increase in the reduction rate. These results show that the influence of the reducing gas flow rate decreases with increasing gas flow rate and that the reduction rate cannot be increased infinitely. A further increase of the gas flow rate leads to a plateau of the reduction rate, because other mechanisms such as the chemical reaction itself become rate limiting.

Fig. 10 depicts the effects of increasing the carbon monoxide gas flow. Only the reduction of  $ZnO$  with carbon monoxide shows a similar tendency to that of hydrogen when the gas flow rate is increased. For  $Fe_2O_3$  and  $ZnOFe_2O_3$ , doubling the gas flow rate only increases the reduction rate by a factor of 1.5, and quadrupling improves the rate only by a factor of 2 up to a reduction rate of about 50%. These results indicate that carbon monoxide is more immobile than hydrogen and the higher concentration gradient resulting from the higher gas flow rate does not affect the reduction rate as significantly as for hydrogen [32]. The smaller increase at higher reduction levels also indicates that diffusion is rate-limiting. The chemical reaction would limit the reaction rate throughout the reduction degree.

Fig. 11 compares the reduction rate for samples at 600 mg and 300 mg at the same relative hydrogen gas flow rate. The rate

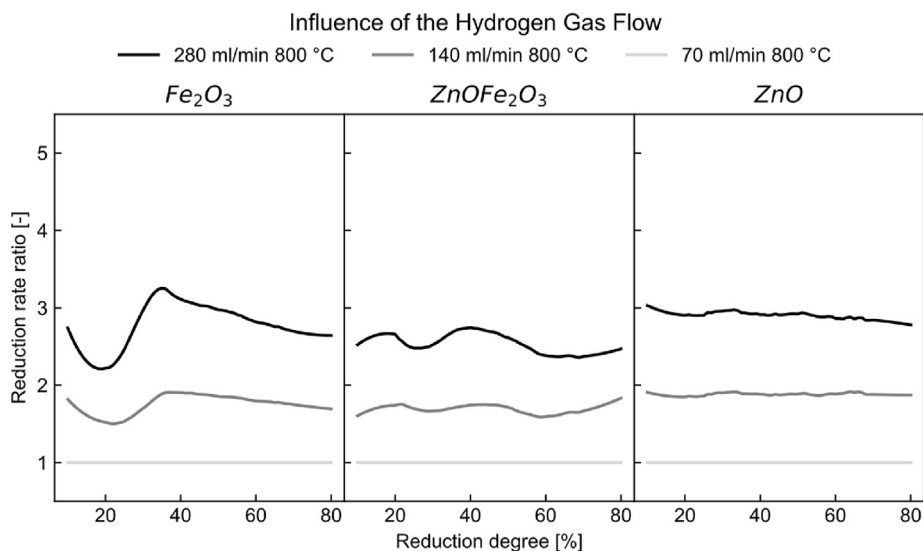


Fig. 9 – Influence of the hydrogen gas flow on the reduction of 300 mg  $\text{Fe}_2\text{O}_3$ ,  $\text{ZnOFe}_2\text{O}_3$  and  $\text{ZnO}$ .

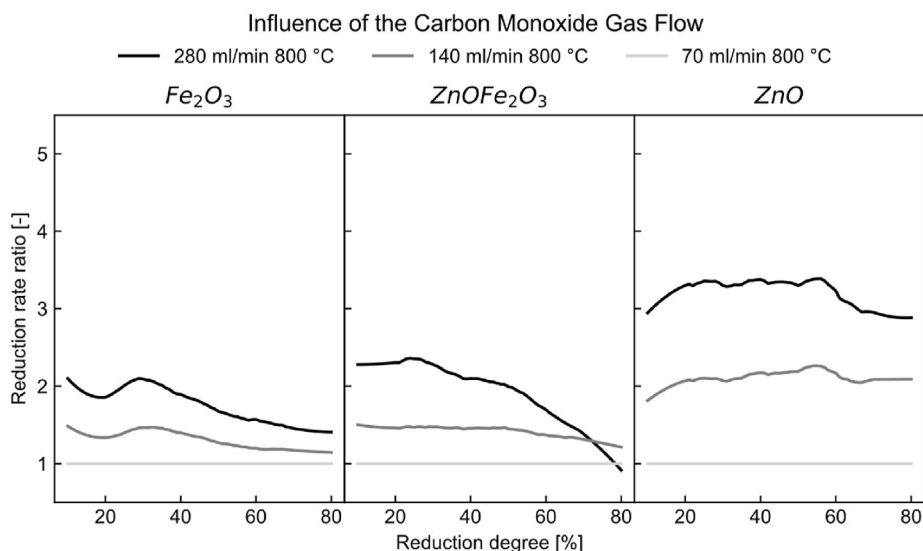


Fig. 10 – Influence of the carbon monoxide gas flow on the reduction of 300 mg  $\text{Fe}_2\text{O}_3$ ,  $\text{ZnOFe}_2\text{O}_3$  and  $\text{ZnO}$ .

ratio is in the range of 0.8 and 1.2 for all comparisons and all oxides. The rate ratios at lower gas flow rates are higher than at the higher gas flow rates. This supports the findings on the rate-limiting mechanism due to the solid, which has already been discussed in detail in Figs. 9 and 10. At the lower gas flow rates, the influence of the gas flow remains more evident and the larger specimen can react faster than the smaller one.

Fig. 12 shows the ratio of reduction rates for specimens with 600 mg and 300 mg at the same specific carbon monoxide gas flow rate. Unlike reduction with hydrogen, doubling the sample size tends to decrease the reduction rate, although the specific gas flow rate doubles simultaneously. Thus, the rate-limiting effect of diffusion is more pronounced for reduction with carbon monoxide. An exception to this trend is the rate ratio for  $\text{ZnO}$  shown by the gray line at the lower gas flow rates. This is due to the fact that the reduction of  $\text{ZnO}$  does not produce a solid product according to equation (3) and equation

(4), so the diffusion effect is as pronounced as for  $\text{Fe}_2\text{O}_3$  and  $\text{ZnOFe}_2\text{O}_3$ .

### 3.3. Discussion of the rate determining mechanisms

The temperature dependency of the reduction rate was hardly detectable for  $\text{Fe}_2\text{O}_3$ . This effect is pronounced for  $\text{ZnO}$ .  $\text{ZnOFe}_2\text{O}_3$  reduction behaves like  $\text{Fe}_2\text{O}_3$  at lower reduction degrees and like  $\text{ZnO}$  at higher reduction degrees in terms of temperature dependency for both reducing agents. These findings correlate with thermodynamic calculations provided in Fig. 13. A detailed explanation of the calculation of the thermodynamic stability fields was done by the authors previously in Ref. [5].

The given experimental results in correlation with previous thermodynamic calculations allow us for the following statements for the different oxides.

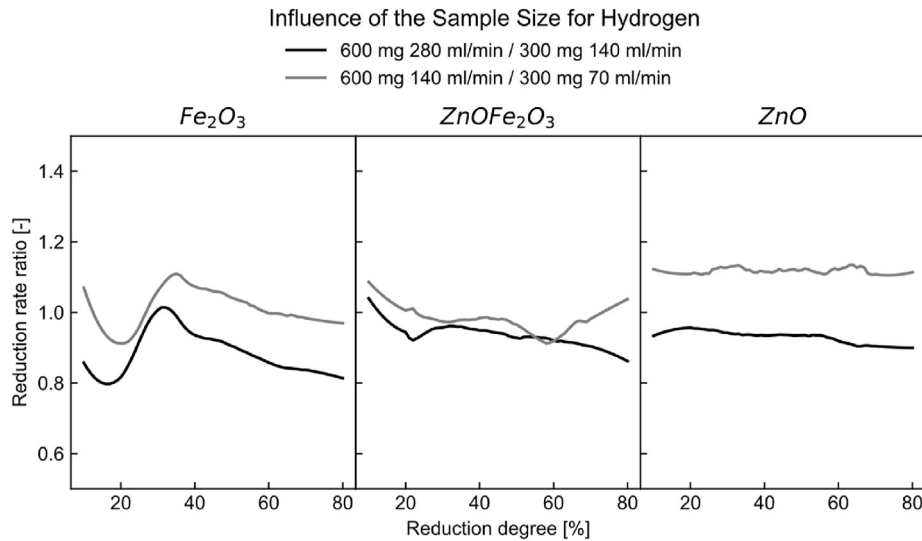


**Fig. 11** – Influence of the sample size on the reduction of  $\text{Fe}_2\text{O}_3$ ,  $\text{ZnOFe}_2\text{O}_3$  and  $\text{ZnO}$  at the same specific hydrogen flow rate.

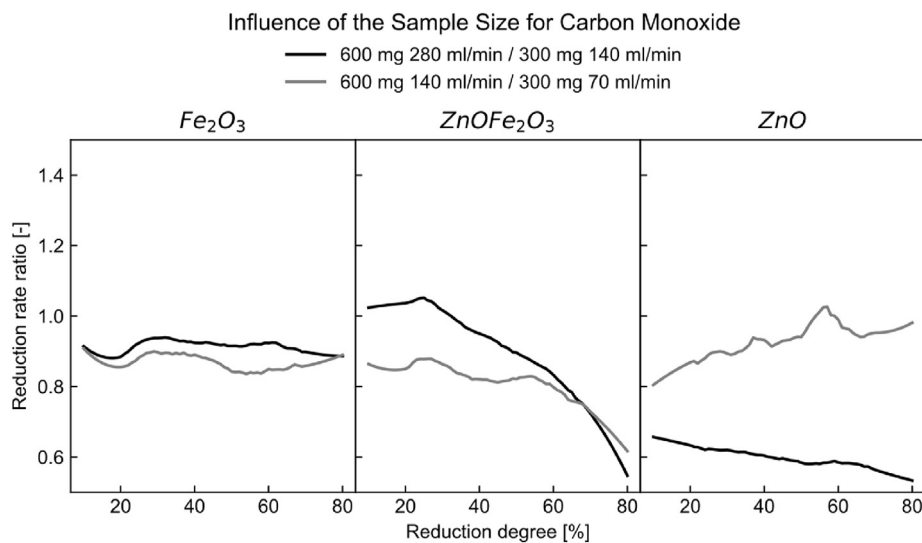


**Fig. 12** – Influence of the sample size on the reduction of  $\text{Fe}_2\text{O}_3$ ,  $\text{ZnOFe}_2\text{O}_3$  and  $\text{ZnO}$  at the same specific carbon monoxide flow rate.

### 3.4. $\text{Fe}_2\text{O}_3$

The results and discussion concerning Figs. 9 and 10 and the not visible temperature dependency for  $\text{Fe}_2\text{O}_3$  in Figs. 7 and 8 indicates that the reduction  $\text{Fe}_2\text{O}_3$  is under diffusional control. Furthermore, hydrogen does not cause the same decrease of the specific surface area as carbon monoxide at the same reduction temperature as given in Table 2. This phenomenon supports diffusional control being the rate limiting factor for  $\text{Fe}_2\text{O}_3$ .

### 3.5. $\text{ZnO}$

According to Figs. 7 and 8 the reduction of  $\text{ZnO}$  is significantly affected by the temperature increase. Additionally, Figs. 9 and 10 exhibit the gas flow dependency of the reduction of  $\text{ZnO}$ , whereby the reduction with carbon monoxide is stronger

dependent on gas flow increase. This means, that the reduction of  $\text{ZnO}$  is notably affected the temperature and the gas flow. Both parameters are responsible for the chemical reaction control. Thus, the chemical reaction controls the kinetics of reduction  $\text{ZnO}$ .

### 3.6. $\text{ZnOFe}_2\text{O}_3$

The reduction of zinc ferrite exhibits both mechanisms (diffusional and chemical control) according to the temperature dependency in Figs. 7 and 8. This means that iron oxide reduction occurs prior to zinc oxide reduction. In a further instance a process development must consider that a selective zinc oxide reduction is only possibly from a thermodynamic point of view as stated in Ref. [5]. At this point it must be pronounced that a selective reduction of  $\text{ZnO}$  was not possible under the chosen experimental conditions and from our point

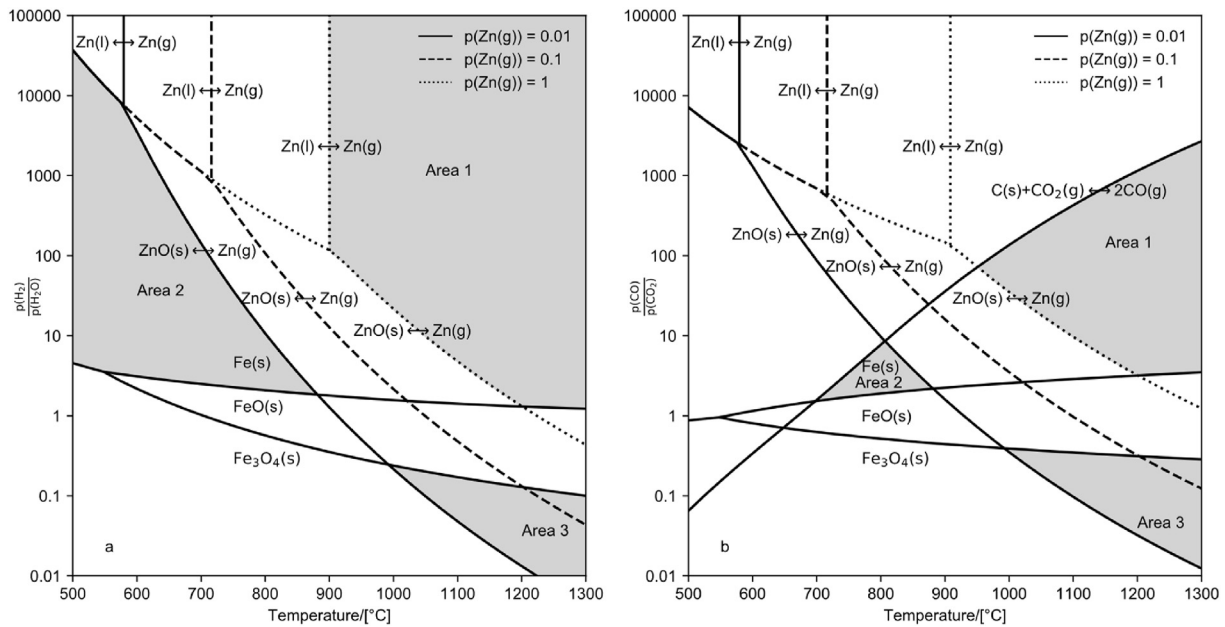


**Fig. 13** – Stability region of Fe, FeO, Fe<sub>3</sub>O<sub>4</sub> and Zn and ZnO as a function of temperature and gas composition for hydrogen and water vapor (a) and carbon monoxide and carbon dioxide (b) [5,33].

of view will not be possible under industrial conditions, when proper reduction kinetics are required.

#### 4. Conclusion

This study is the first work to provide a comprehensive dataset of the reduction rates for the main oxides in electric arc furnace dust (EAFD). For this purpose, the main oxides Fe<sub>2</sub>O<sub>3</sub>, ZnOFe<sub>2</sub>O<sub>3</sub> and ZnO were reduced with hydrogen and carbon monoxide in an individual thermogravimetric analyzing (TGA) system. Regardless of the reducing agent, the reduction of ZnO is rate-limiting for the treatment of EAFD. The reduction of Fe<sub>2</sub>O<sub>3</sub> is stepwise, producing intermediate Fe<sub>3</sub>O<sub>4</sub> and FeO. The stepwise reduction is also observed for ZnOFe<sub>2</sub>O<sub>3</sub>, but not for ZnO. The kinetic advantage of hydrogen accounts for a factor of 2.5 for Fe<sub>2</sub>O<sub>3</sub> and 2 for ZnOFe<sub>2</sub>O<sub>3</sub>. In the case of ZnO, hydrogen only leads to a kinetic advantage by a factor of 1.5. Regardless of the reducing agent, an increase in temperature leads to better reduction kinetics. This effect is most pronounced for ZnO and decreases for ZnOFe<sub>2</sub>O<sub>3</sub>. For Fe<sub>2</sub>O<sub>3</sub>, the temperature dependence almost disappears. A quadrupling of the gas flow leads to a tripling of the rate for all oxides with hydrogen and only for ZnO when carbon monoxide is used. This suggests that the rate-determining mechanism originating from the solid (gas diffusion in the layer) changes when the gas rate is increased, and that gas diffusion through the solid layer is innately more influential for ZnOFe<sub>2</sub>O<sub>3</sub> and Fe<sub>2</sub>O<sub>3</sub>. The decrease of the specific surface area cause by carbon monoxide and for Fe<sub>2</sub>O<sub>3</sub> is greater than caused by hydrogen and for ZnOFe<sub>2</sub>O<sub>3</sub>. These findings are in line with the kinetic results gained in the TGA. Additionally, the experimental setup with the different gas flow change rates and the different temperature allows for the following

statement: Independently of the reducing agent the rate limiting mechanism for Fe<sub>2</sub>O<sub>3</sub> is diffusion, while the reduction of ZnO is limited by the chemical reaction. Importantly for process design for EAFD recycling, hydrogen-based reduction is strongly influenced by the gas flow rate. Therefore, reactors for hydrogen-based technologies must consider that a higher gas flow rate allows for better kinetics. The confirmation of the kinetic advantage of hydrogen-based reduction indicates the high potential of hydrogen-based reduction.

Furthermore, these results indicate that further knowledge, especially with respect to upscaling the kinetic results, needs to be gained.

#### Declaration of competing interest

The authors declare that they have no known competing financial interests or personal relationships that could have appeared to influence the work reported in this paper.

#### Acknowledgement

This work was supported by the Austrian Research Promotion Agency.

#### REFERENCES

- [1] World Steel Association. *Steel's contribution to a low carbon future and climate resilient societies*. 2020.
- [2] Xylia Maria, et al. *Worldwide resource efficient steel production*. 2016. Stockholm.
- [3] Worldsteel Association. *World steel in figures 2020*. 2021.

- [4] Guézennec A-G, et al. Dust formation in electric arc furnace: birth of the particles. *Powder Technol* 2005;157:2–11.
- [5] Brandner U, Antrekowitsch J, Leuchtenmueller M. A review on the fundamentals of hydrogen-based reduction and recycling concepts for electric arc furnace dust extended by a novel conceptualization. *Int J Hydrogen Energy* 2021;46:31894–902.
- [6] Remus R, et al. Best available techniques (BAT) reference document for iron and steel production. In: EUR (Luxembourg), band: 25521. Luxembourg: Publications Office; 2013.
- [7] Stewart DJ, Barron AR. Pyrometallurgical removal of zinc from basic oxygen steelmaking dust – a review of best available technology. *Resour Conserv Recycl* 2020;157:104746.
- [8] A European Green Deal. Internet. [https://ec.europa.eu/info/strategy/priorities-2019-2024/european-green-deal\\_en](https://ec.europa.eu/info/strategy/priorities-2019-2024/european-green-deal_en). Zugriff: 09.08.2021.
- [9] Oh J, Noh D. The reduction kinetics of hematite particles in H<sub>2</sub> and CO atmospheres. *Fuel* 2017;196:144–53.
- [10] Tong LF. Reduction mechanisms and behaviour of zinc ferrite—Part 1: pure ZnFe<sub>2</sub>O<sub>4</sub>. *Miner Process Extr Metall (IMM Trans Sect C)* 2001;110:14–24.
- [11] Tong LF. Reduction mechanisms and behaviour of zinc ferrite—Part 2: ZnFe<sub>2</sub>O<sub>4</sub> solid solutions. *Miner Process Extr Metall (IMM Trans Sect C)* 2001;110:123–32.
- [12] Tong LF, Hayes P. Mechanisms of the reduction of zinc ferrites in H<sub>2</sub>/N<sub>2</sub> gas mixtures. *Miner Process Extr Metall Rev* 2006;28:127–57.
- [13] Junca E, et al. Synthetic zinc ferrite reduction by means of mixtures containing hydrogen and carbon monoxide. *J Therm Anal Calorim* 2016;123:631–41.
- [14] Kinetics of the Reduction of Iron Ore: tokuda et al.
- [15] Zuo H, et al. Reduction kinetics of iron oxide pellets with H<sub>2</sub> and CO mixtures. *Int J Miner Metall Mater* 2015;22:688–96.
- [16] Sofilić T, et al. Characterization of steel mill electric-arc furnace dust. *J Hazard Mater* 2004;109:59–70.
- [17] Brandner U. et al.: A tailor-made experimental setup for thermogravimetric analysis of the hydrogen- and carbon monoxide-based reduction of iron (III) oxide (Fe<sub>2</sub>O<sub>3</sub>) and zinc ferrite (ZnOFe<sub>2</sub>O<sub>3</sub>): TMS 2022 151st annual meeting & exhibition supplemental proceedings. Cham: Springer International Publishing, 917–926.
- [18] Brunauer S, PH. Emmett und E. Teller: adsorption of Gases in Multimolecular Layers. *J Am Chem Soc* 1938;60:309–19.
- [19] Virtanen P, et al. SciPy 1.0: fundamental algorithms for scientific computing in Python. *Nat Methods* 2020;17:261–72.
- [20] Harris CR, et al. Array programming with NumPy. *Nature* 2020;585:357–62.
- [21] Spreitzer D. und J. Schenk: iron Ore Reduction by Hydrogen Using a Laboratory Scale Fluidized Bed Reactor: kinetic Investigation—experimental Setup and Method for Determination. *Metall Mater Trans B* 2019;50:2471–84.
- [22] Barde AA, Klausner JF, Mei R. Solid state reaction kinetics of iron oxide reduction using hydrogen as a reducing agent. *Int J Hydrogen Energy* 2016;41:10103–19.
- [23] Abu Tahari MN, et al. Influence of hydrogen and carbon monoxide on reduction behavior of iron oxide at high temperature: effect on reduction gas concentrations. *Int J Hydrogen Energy* 2020;46:24791–805.
- [24] Qu Y, et al. Kinetic characterization of flash reduction process of hematite ore fines under hydrogen atmosphere. *Int J Hydrogen Energy* 2020;45:31481–93.
- [25] Pineau A, Kanari N, Gaballah I. Kinetics of reduction of iron oxides by H<sub>2</sub> Part I. *Thermochim Acta* 2006;447:89–100.
- [26] Pineau A, Kanari N, Gaballah I. Kinetics of reduction of iron oxides by H<sub>2</sub> Part II. *Thermochim Acta* 2007;456:75–88.
- [27] Junca E, et al. Reduction of electric arc furnace dust pellets by mixture containing hydrogen. *REM - International Engineering Journal* 2019;72:55–61.
- [28] Junca E, et al. Application of stepwise isothermal analysis method in the kinetic study of reduction of basic oxygen furnace dust. *J Therm Anal Calorim* 2015;120:1913–9.
- [29] Junca E, et al. Reduction of electric arc furnace dust pellets by simulated reformed natural gas. *J Therm Anal Calorim* 2016;126:1889–97.
- [30] Junca E, et al. Kinetic investigation of synthetic zinc ferrite reduction by hydrogen. *J Therm Anal Calorim* 2017;129:1215–23.
- [31] Spreitzer D. und J. Schenk: reduction of Iron Oxides with Hydrogen—a Review. *Steel Res Int* 2019;90:1–17.
- [32] Vyazovkin S, et al. ICTAC Kinetics Committee recommendations for performing kinetic computations on thermal analysis data. *Thermochim Acta* 2011;520:1–19.
- [33] Bale CW, et al. FactSage thermochemical software and databases, 2010–2016. *Calphad* 2016;54:35–53.